

Bicyclobutane Carboxylic Amide as a Cysteine-Directed Strained Electrophile for Selective Targeting of Proteins

Keisuke Tokunaga, Mami Sato, Keiko Kuwata, Chizuru Miura, Hirokazu Fuchida, Naoya Matsunaga, Satoru Koyanagi, Shigehiro Ohdo, Naoya Shindo,* and Akio Ojida*



Cite This: <https://dx.doi.org/10.1021/jacs.0c07490>



Read Online

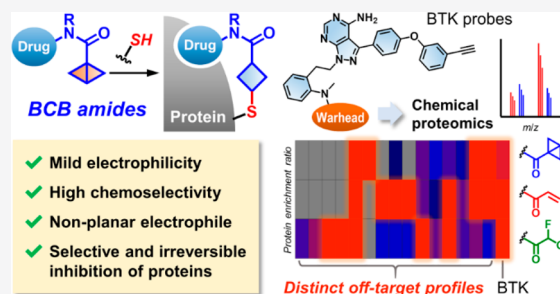
ACCESS |

Metrics & More

Article Recommendations

Supporting Information

ABSTRACT: Expanding the repertoire of electrophiles with unique reactivity features would facilitate the development of covalent inhibitors with desirable reactivity profiles. We herein introduce bicyclo[1.1.0]butane (BCB) carboxylic amide as a new class of thiol-reactive electrophiles for selective and irreversible inhibition of targeted proteins. We first streamlined the synthetic routes to generate a variety of BCB amides. The strain-driven nucleophilic addition to BCB amides proceeded chemoselectively with cysteine thiols under neutral aqueous conditions, the rate of which was significantly slower than that of acrylamide. This reactivity profile of BCB amide was successfully exploited to develop covalent ligands targeting Bruton's tyrosine kinase (BTK). By tuning BCB amide reactivity and optimizing its disposition on the ligand, we obtained a selective covalent inhibitor of BTK. The in-gel activity-based protein profiling and mass spectrometry-based chemical proteomics revealed that the selected BCB amide had a higher target selectivity for BTK in human cells than did a Michael acceptor probe. Further chemical proteomic study revealed that BTK probes bearing different classes of electrophiles exhibited distinct off-target profiles. This result suggests that incorporation of BCB amide as a cysteine-directed electrophile could expand the capability to develop covalent inhibitors with the desired proteome reactivity profile.



INTRODUCTION

Small molecules with an electrophilic reactive group can form a covalent bond with nucleophilic amino acid residues of proteins. This irreversible mode of action allows for durable and specific functional regulation of the targeted protein, offering therapeutic advantages, such as sustained and enhanced drug efficacy,¹ isoform-selective inhibition,² and the overcoming of acquired drug resistance.³ Despite the concerns about latent toxicity of covalent binders due to their potentially indiscriminate reactivity with biomolecules,⁴ recent successes in the development of targeted covalent inhibitors (TCIs) demonstrate the benefits of irreversible inhibition of therapeutically relevant proteins.⁵ For example, several TCIs have been clinically used for the inactivation of cancer-associated tyrosine kinases, such as epidermal growth factor receptor (EGFR) and Bruton's tyrosine kinase (BTK).^{3,6} The utility of the covalent inhibition has been also confirmed by the recent efforts to develop TCIs targeting the KRAS protein with an oncogenic G12C mutation. This protein had been considered "undrugable" due to the lack of an appropriate binding pocket to accommodate small molecule ligands.⁷

During TCI design, the reactivity of the electrophilic group (warhead) should be carefully tuned to minimize off-target reactions, while maintaining sufficient reactivity with the targeted protein. The Michael acceptors, such as acrylamide,

are the most prevalent cysteine-directed warheads employed in various TCIs (Figure 1A). Chloroacetamide represents another established class of cysteine-directed warheads. It has been widely used in covalent ligand discovery based on the electrophile-fragment screening.⁸ However, the rather high reactivity of chloroacetamide might not be suitable for therapeutic applications due to the risk of off-target reactions. We have recently introduced chlorofluoroacetamide (CFA) as a less reactive α -haloacetamide and demonstrated its utility in the target-specific inhibition of protein kinases.⁹ Recently, hetero-aromatic sulfones and sulfoxides, which react with thiols via nucleophilic aromatic substitution (S_NAr) reactions, have also been reported as cysteine-directed electrophiles.¹⁰

It is reasonable to assume that the reactivity profile of a TCI can be regulated by multiple facets of the adopted electrophile, including intrinsic electrophilicity, mode of reaction, chemoselectivity, molecular shape, and reversibility of the covalent engagement. Introduction of new classes of electrophiles as

Received: July 12, 2020

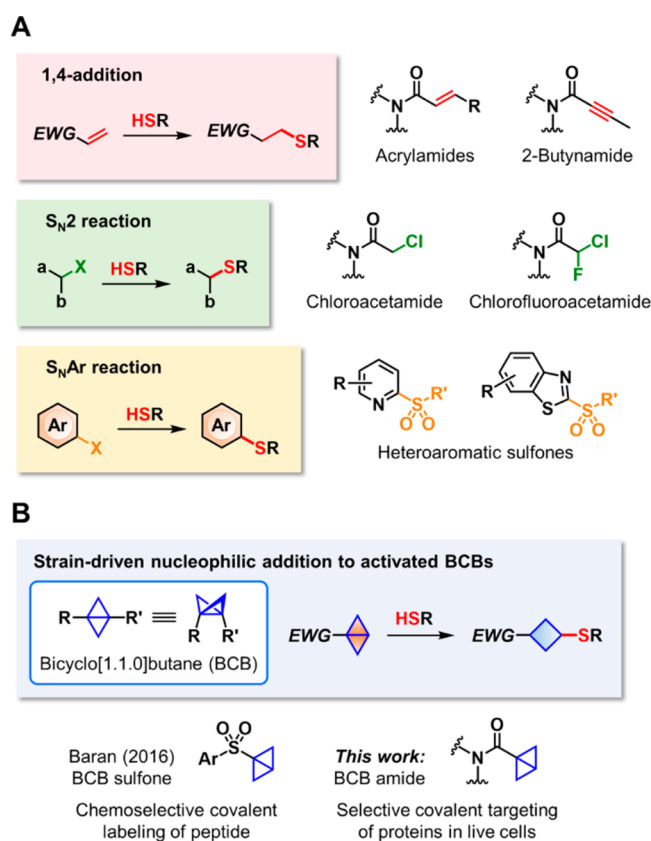


Figure 1. Chemistry for cysteine-directed bioconjugation. (A) Prevalent reactions and representative electrophiles. (B) Strain-driven nucleophilic addition to activated bicyclo[1.1.0]butanes (BCBs) utilized in this work. EWG, electron-withdrawing group.

reactive warheads, therefore, would facilitate the development of covalent inhibitors with desirable reactivity profiles. In medicinal chemistry and chemical biology research, three- or four-membered rings have been utilized as a unique class of electrophiles with strain-enabled reactivities.^{11–13} Among the highly strained carbocyclic systems,¹⁴ we focused on bicyclo[1.1.0]butane (BCB)¹⁵ derivatives as a less explored class of strained electrophiles. BCB has a unique structure, in which the cyclobutane ring is folded into a puckered, butterfly-like shape by the bridging carbon–carbon bond. Despite the

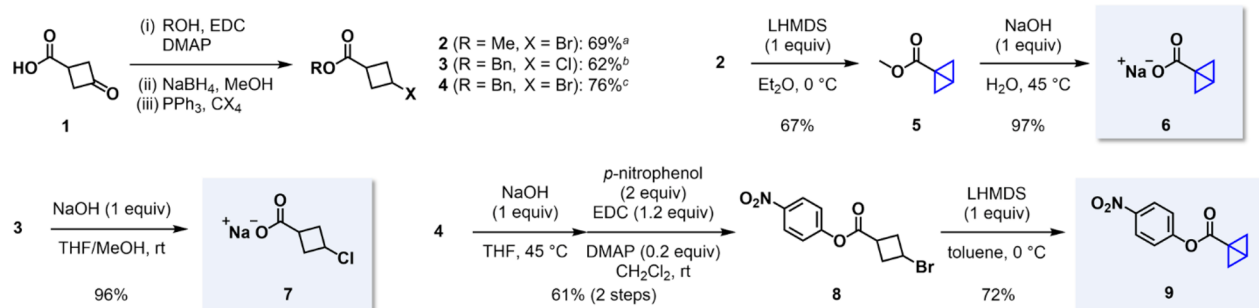
high strain energy of the ring system (~ 66 kcal/mol),¹⁶ BCB is stable under aqueous conditions and can be constructed by the enzyme reactions.¹⁷ The unique strain-driven reactivity of BCB has been harnessed in diverse types of reactions, such as cycloisomerization,¹⁸ carbopalladation,¹⁹ and radical-mediated reactions.²⁰ BCB also undergoes nucleophilic ring-opening when activated by an electron-withdrawing group (EWG) at the bridgehead carbon.²¹ Recently, Baran et al. have reported the potential utility of BCB sulfones as a cysteine-directed covalent warhead in the chemoselective reaction with peptides in aqueous media (Figure 1B).²² However, to the best of our knowledge, BCB derivatives have not yet been used for covalent targeting of proteins in live cell conditions; moreover, their proteome-wide reactivity profiles have not yet been explored. In this Article, we mainly focused on BCB carboxylic amides and examined their utility as a reactive warhead of covalent inhibitors. We envisioned that BCB amides would be suitable for selective targeting of proteins by virtue of the weak and tunable activating effect of the amide carbonyl group, and installation of a BCB ring to drugs through an amide bond would benefit flexible molecular design (Figure 1B). Although BCB amides have been occasionally reported in the literature,^{20b,21a,d,23} systematic studies on their synthesis and reactivity are not available.

In this report, we present BCB amide as a new class of cysteine-directed electrophiles useful for TCI design. BCB amide is stable under neutral aqueous conditions, and it shows chemoselective and tunable reactivity toward cysteine thiol. We demonstrated the utility of BCB amide in the development of a covalent inhibitor for BTK. The in-gel activity-based protein profiling (ABPP) and mass spectrometry (MS)-based chemical proteomics revealed that the BCB amide probe exhibited a higher target selectivity for BTK than did a Michael acceptor probe. Further proteomic study revealed that BTK inhibitors possessing different classes of electrophiles (BCB amide, acrylamide, and CFA) show distinct off-target profiles. This finding suggests the importance of expanding the scope of thiol-reactive electrophiles, which would enable the development of novel TCIs with desirable proteome reactivity profiles.

RESULTS AND DISCUSSION

Synthesis of BCB Amides. As a common synthetic approach to generate a highly strained BCB ring, we employed

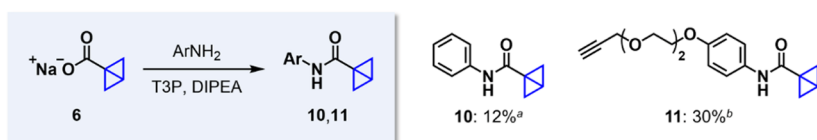
Scheme 1. Building Blocks for BCB Amide Synthesis^a



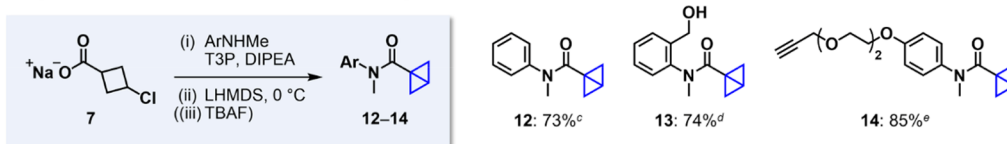
^a(a) Reaction conditions: (i) 1 (1.0 equiv), MeOH (1.5 equiv), EDC-HCl (1.3 equiv), DMAP (0.2 equiv), CH₂Cl₂, rt; (ii) NaBH₄ (0.6 equiv), MeOH, 0 °C; (iii) PPh₃ (2.8 equiv), CBr₄ (2.8 equiv), LiBr (2.8 equiv), THF, rt (69% over three steps). (b) Conditions: (i) 1 (1.1 equiv), BnOH (1 equiv), EDC-HCl (1.1 equiv), DMAP (0.2 equiv), CH₂Cl₂, rt; (ii) NaBH₄ (0.5 equiv), MeOH, 0 °C; (iii) PPh₃ (2.5 equiv), CCl₄ (solvent), reflux (62% over three steps). (c) Conditions: (i) 1 (1.1 equiv), BnOH (1 equiv), EDC-HCl (1.2 equiv), DMAP (0.2 equiv), CH₂Cl₂, rt; (ii) NaBH₄ (0.5 equiv), MeOH, 0 °C; (iii) PPh₃ (1.8 equiv), CBr₄ (1.8 equiv), LiBr (1.9 equiv), THF, 45 °C (76% over three steps).

Scheme 2. Synthesis of BCB Amides^a

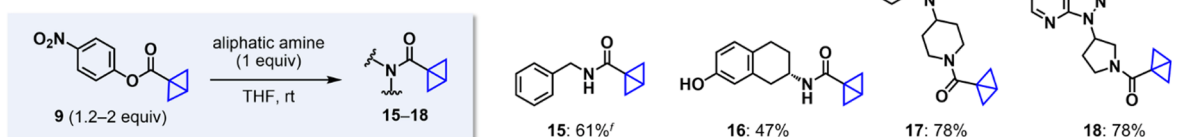
A. Preparation of BCB amides from aromatic primary amines



B. Preparation of BCB amides from aromatic secondary amines



C. Preparation of BCB amides from aliphatic amines



^a(a) Reaction conditions: **6** (2.0 equiv), aniline (1.0 equiv), T3P (3.0 equiv), DIPEA (3.0 equiv), DMF, rt, 3 h. (b) Conditions: **6** (1.4 equiv), ArNH₂ (1.0 equiv), T3P (1.5 equiv), DIPEA (3.1 equiv), CH₂Cl₂, rt, 16 h. (c) Conditions: (i) **7** (1.9 equiv), ArNHMe (1.0 equiv), T3P (3.0 equiv), DIPEA (3.0 equiv), DMF, rt, 12 h; (ii) LHMDS (1.1 equiv), THF, 0 °C, 1 h (73% over two steps). (d) Conditions: (i) **7** (1.1 equiv), ArNHMe (1.0 equiv), T3P (1.5 equiv), DIPEA (3.0 equiv), DMF, rt, 12 h; (ii) LHMDS (1.2 equiv), THF, 0 °C, 2.5 h; (iii) TBAF (1.2 equiv), THF, 0 °C, 30 min (74% over three steps). (e) Conditions: (i) **7** (1.2 equiv), ArNHMe (1.0 equiv), T3P (1.5 equiv), DIPEA (3.0 equiv), DMF, rt, 4 h; (ii) LHMDS (1.5 equiv), THF, 0 °C, 2 h; (iii) TBAF (1.5 equiv), THF, 0 °C, 30 min (85% over three steps). (f) 1.0 equiv of **9** was treated with 1.5 equiv of benzylamine.

A. Nucleophilic addition to activated BCBs under basic conditions in DMF/H₂O

Entry	BCB	EWG	NuH	Time (h)	Product	Yield (%)	cis/trans
1	12	-CONMePh	H-Cys-OMe	12	21	60	71:29
2 ^a	12	-CONMePh	PhSH	1	22	70	70:30
3 ^a	12	-CONMePh	HOCH ₂ CH ₂ SH	4	23	67	67:33
4 ^a	19	-CO ₂ Bn	PhSH	0.3	24	86	69:31
5 ^a	20	-SO ₂ Ph	PhSH	1	25	85	14:86
6	12	-CONMePh	H-Lys-OMe	12	—	NR	—
7	12	-CONMePh	H-Ser-OMe	12	—	NR	—
8	12	-CONMePh	H-His-OMe	12	—	NR	—
9	12	-CONMePh	H-Tyr-OMe	12	—	NR	—
10	12	-CONMePh	H-Trp-OMe	12	—	NR	—

B. Reactivity of electrophiles toward GSH under physiological conditions

Entry	Electrophile	<i>t</i> _{1/2} (h)
1	10	32.7
2	12	79.0
3	15	136.3
4	26	2.5
5	20	11.8
6	27	1.2
7	28	40.7

Figure 2. In vitro electrophilic reactivity of BCB amides in comparison with that of other electrophiles. (A) Reactions of activated BCBs with nucleophiles under basic conditions in DMF/H₂O. Reaction conditions: BCB derivative (0.1 M, 1.0 equiv), nucleophile (NuH) (1.0 equiv), K₂CO₃ (1.0 equiv) in DMF/H₂O (1:1) at ambient temperature under N₂ atmosphere. (a) 2.0 equiv of the designated thiol was used. NR, no reaction. (B) Evaluation of the half-time (*t*_{1/2}) of the reaction between electrophiles and glutathione (GSH). Reaction conditions: electrophile (1 mM) and GSH (10 mM) in 100 mM potassium phosphate buffer (pH 7.2) containing 10% DMF at 37 °C under N₂ atmosphere.

the base-mediated intramolecular cyclization of 3-halocyclobutane carboxylic esters and amides according to the first synthesis of a BCB ester reported by Wiberg.²⁴ We streamlined the synthesis of BCB amides by using the three building blocks **6**, **7**, and **9**, all of which can be easily prepared from the commercially available carboxylic acid **1** (Scheme 1). Carboxylate salt **6** was used for amide coupling of the primary aromatic amines to obtain BCB amides **10** and **11** by using propylphosphonic

anhydride (T3P) as the condensation reagent (Scheme 2A). Low yields of these products can be ascribed to the sterically bulky quaternary bridgehead carbon of BCB ring that hampers the reaction at the carbonyl carbon of **6**. By contrast, amide coupling of the sterically less-congested carboxylate salt **7** with the secondary aromatic amines proceeded smoothly, yielding the corresponding amides. The subsequent treatment with lithium bis(trimethylsilyl)amide (LHMDS) afforded BCB

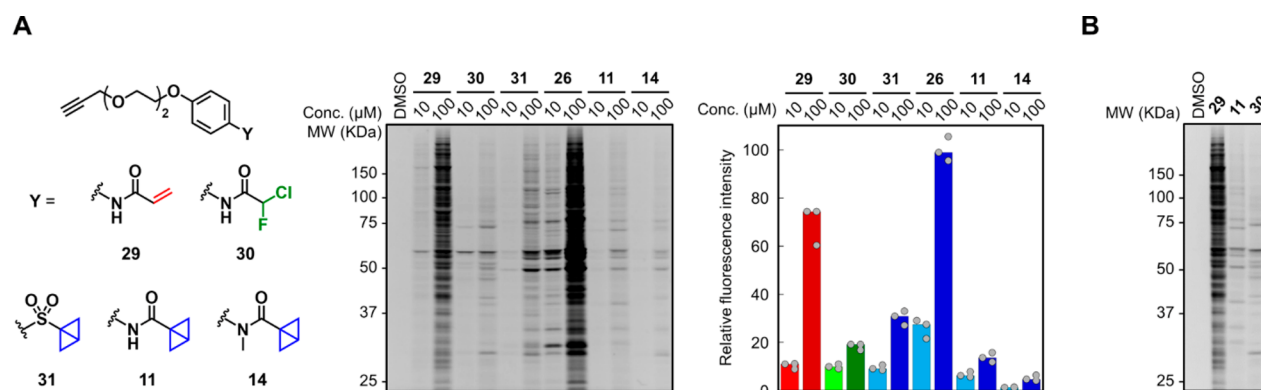


Figure 3. Evaluation of the proteome-wide reactivity of the alkynylated electrophiles. (A) Chemical structures of alkynylated probes and their reactivity profiles in living cells. A431 cells were treated with the designated probes (10 or 100 μM , 6 h) and analyzed by in-gel ABPP (middle panel). The right panel shows the relative fluorescence intensity of each lane in the gel. The fluorescence intensity of the lane with 100 μM **26** is set to an arbitrary value of 100. The bar height represents the median of three independent experiments. (B) A side-by-side comparison of the band patterns upon the treatment of A431 cell with acrylamide **29**, BCB amide **11**, or CFA **30** in the in-gel ABPP analysis (100 μM , 6 h).

amides **12**–**14** in good yields (Scheme 2B). The activated 4-nitrophenyl BCB ester **9** was used for the coupling with primary and secondary aliphatic amines to furnish BCB amides **15**–**18**. The reactions proceeded smoothly at ambient temperature without any external reagent, enabling high-throughput and late-stage synthesis of BCB amides from drug-like aliphatic amines (Scheme 2C).

Electrophilic Reactivity of BCB Amides. With a series of BCB amides in hand, we investigated their reactivity as strained electrophiles. Under basic conditions in a mixed aqueous/organic solvent system (K_2CO_3 in 1:1 DMF/ H_2O), BCB amide **12** reacted readily with thiols to furnish the corresponding adducts **21**–**23** as mixtures of diastereomers at a ratio of $\sim 7:3$ (Figure 2A, entries 1–3). The major product was assigned as *cis*-1,3-disubstituted cyclobutane by the ^1H NMR analysis (see the Supporting Information). The *cis*-selectivity (*cis/trans* = 69:31) was also observed in the reaction of BCB ester **19** with thiophenol (entry 4). Interestingly, BCB sulfone **20** showed a reversed diastereoselectivity in the reaction with thiophenol to provide *trans*-**25** as the major isomer (*cis/trans* = 14:86). The change in the diastereoselectivity could be explained by the different stabilizing effect of the EWG on the transiently formed carbanion according to the report by Hoz.²⁵ BCB amide appeared to be a chemoselective electrophile toward thiol groups, as **12** did not react with nucleophilic amino acids (lysine, serine, histidine, tyrosine, and tryptophan) other than cysteine even under the basic reaction conditions (entries 6–10).

We next evaluated the reactivity of BCB derivatives toward glutathione (GSH) under the neutral aqueous conditions (100 mM potassium phosphate buffer, pH 7.2, 37 $^\circ\text{C}$) (Figures 2B and S1). The reaction with an excess of GSH (10 equiv) was monitored by HPLC, and the formation of the corresponding GSH adduct was confirmed by electrospray ionization mass spectrometry. The first-order reaction kinetic analysis showed that the half-times ($t_{1/2}$) of the reactions of BCB amides **10** and **12** with GSH were 32.7 and 79.0 h, respectively. These reaction rates were much slower than that of acrylamide **27** ($t_{1/2}$ = 1.2 h), but comparable to that of CFA **28** ($t_{1/2}$ = 40.7 h). The moderate to weak reactivity of these BCB amides would be suitable for the development of target-specific covalent inhibitors. Aliphatic amine-derived BCB amide **15** showed a slower reaction rate ($t_{1/2}$ = 136.3 h) as compared to those of **10** and **12**. Interestingly, BCB ester **26** exhibited high reactivity ($t_{1/2}$ = 2.5 h) comparable

to that of acrylamide **27**, whereas BCB sulfone **20** showed a slightly higher reactivity ($t_{1/2}$ = 11.8 h) than did compounds **10** and **12**. Of note, all tested BCB derivatives were stable for days in the absence of GSH (Figure S2). Taken together, these reaction kinetics data suggest that the thiol reactivity of activated BCB is tunable in a wide range, depending on the connected EWG. According to previous studies, this difference in reactivity would be a result of a combination of multiple factors, including electronic and steric effects of the substituent on the BCB ring.^{22,25,26}

We next assessed proteome-wide reactivity profiles of BCB amide and other electrophiles in living cells by gel-based ABPP (Figure 3). A431 cells were treated with alkynylated probes **11**, **14**, **26**, and **29**–**31** (10 or 100 μM , 37 $^\circ\text{C}$, 6 h), and the labeled proteins were conjugated to rhodamine-azide (Rho- N_3) by copper-catalyzed azide–alkyne cycloaddition (CuAAC) for in-gel fluorescence analysis. Because these probes share the same alkynylated benzene scaffold, we expected that their reactivity profiles would mainly reflect intrinsic physicochemical properties of the appended electrophile. The fluorescence gel image showed that all of the probes reacted with cellular proteins in a concentration-dependent manner (Figure 3A). Acrylamide **29** and BCB ester **26** exhibited much higher proteome-wide reactivities than did other probes. This reactivity trend is consistent with that observed in the *in vitro* reactivity experiment with GSH (Figure 2B). The same trend was also observed in the labeling experiment using A431 cell lysate (Figure S3). The higher reactivity of **26** as compared to **29** (both under live cell and lysate conditions) might be ascribed to the high lipophilicity of the BCB ester moiety, which likely enhanced the promiscuous binding to cellular proteins. It should be noted that BCB amides **11** and **14** displayed low proteome-wide reactivity even at 100 μM , the extent of which was comparable to that of CFA probe **30**. Notably, acrylamide **29**, CFA **30**, and BCB amide **11** displayed different band patterns in the gel, indicating that each probe possessed distinct proteome reactivity. This point is more clearly visualized in a side-by-side comparison gel image (Figure 3B). Overall, our data suggest that BCB amide functions as a cysteine-directed electrophile with moderate to weak reactivity suitable for in-cell protein labeling and shows a unique proteome selectivity different from that of the Michael acceptor and CFA-type covalent probes.

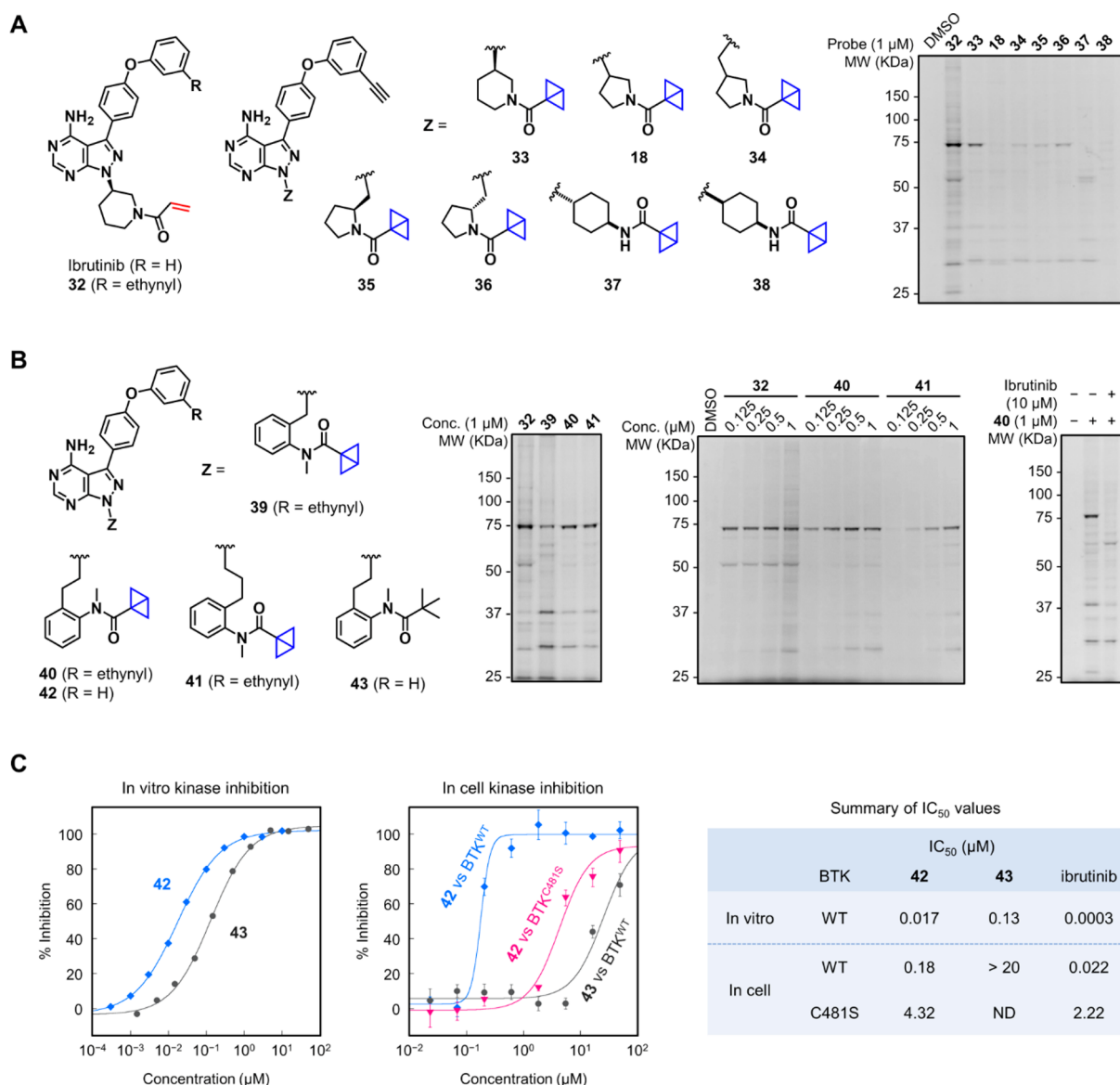


Figure 4. Development of BCB amide-based covalent BTK inhibitors. (A) Reactivity profiles of aliphatic BCB amide probes in Ramos cells (1 μM , 4 h) analyzed by in-gel ABPP. (B) Reactivity profiles of aromatic BCB amide probes toward BTK in Ramos cells. Left: Comparison of reactivities of probes 39–41 (1 μM , 4 h) with different alkyl linkers. Middle: Concentration-dependent reactivity profiles of probes 32, 40, and 41 (0.125–1 μM , 4 h). Right: Competitive protein labeling in Ramos cells by 40 and ibrutinib. (C) Biological activities of BTK inhibitors. Left: In vitro kinase inhibitory activity of BCB amide 42 and control compound 43 against BTK. Each plot represents the mean of two independent experiments. Middle: In-cell inhibitory activity of the compounds against BTK autophosphorylation. Data are presented as the mean \pm standard deviation of experiments performed in triplicate. Right: Summary of IC_{50} values of 42, 43, and ibrutinib in different experiments. WT, wild type; ND, not determined.

Development of BCB Amide-Based BTK Inhibitors. To demonstrate the utility of BCB amide in TCI development, we designed covalent inhibitors targeting protein tyrosine kinase BTK and evaluated their reactivity profiles (Figure 4). Currently, two irreversible BTK inhibitors, ibrutinib and acalabrutinib, have been clinically approved by the FDA for use in the treatment of B-cell malignancies.⁶ These TCIs contain a Michael acceptor moiety as warhead and irreversibly bind to BTK via the covalent modification of Cys481. On the basis of the molecular architecture of ibrutinib, we first synthesized a series of BCB amides, 18, 33–38, each harboring a different aliphatic amine linker connecting the BCB amide moiety to the pyrazolo[3,4-*d*]pyrimidine scaffold (Figures 4A and S4). In the in-gel ABPP analysis in Ramos cells (1 μM probe, 37 $^{\circ}\text{C}$, 4 h), the control Michael acceptor probe 32, a validated alkynylated

analogue of ibrutinib,²⁷ exhibited a strong fluorescent band of BTK at 77 kDa (Figure 4A). In contrast, the aliphatic BCB amide probes showed moderate to weak labeling of the BTK band. This result was intriguing because the aliphatic BCB amides can serve as a reactive warhead of covalent binders despite their very weak thiol reactivity (Figure 2B). Although probe 33 was the one that reacted with BTK most efficiently among the series, its labeling ability apparently became lower than that of 32 at the lower concentration range (0.125–0.5 μM) (Figure S5). To improve the covalent labeling efficiency, we next designed probes 39–41 containing a more reactive aromatic BCB amide, in which a flexible alkyl chain was adopted as the linker to orient the BCB amide toward Cys481.²⁸ We found that BCB amides 40 and 41 exhibited improved reactivities toward BTK in Ramos cells (Figure 4B, left panel).

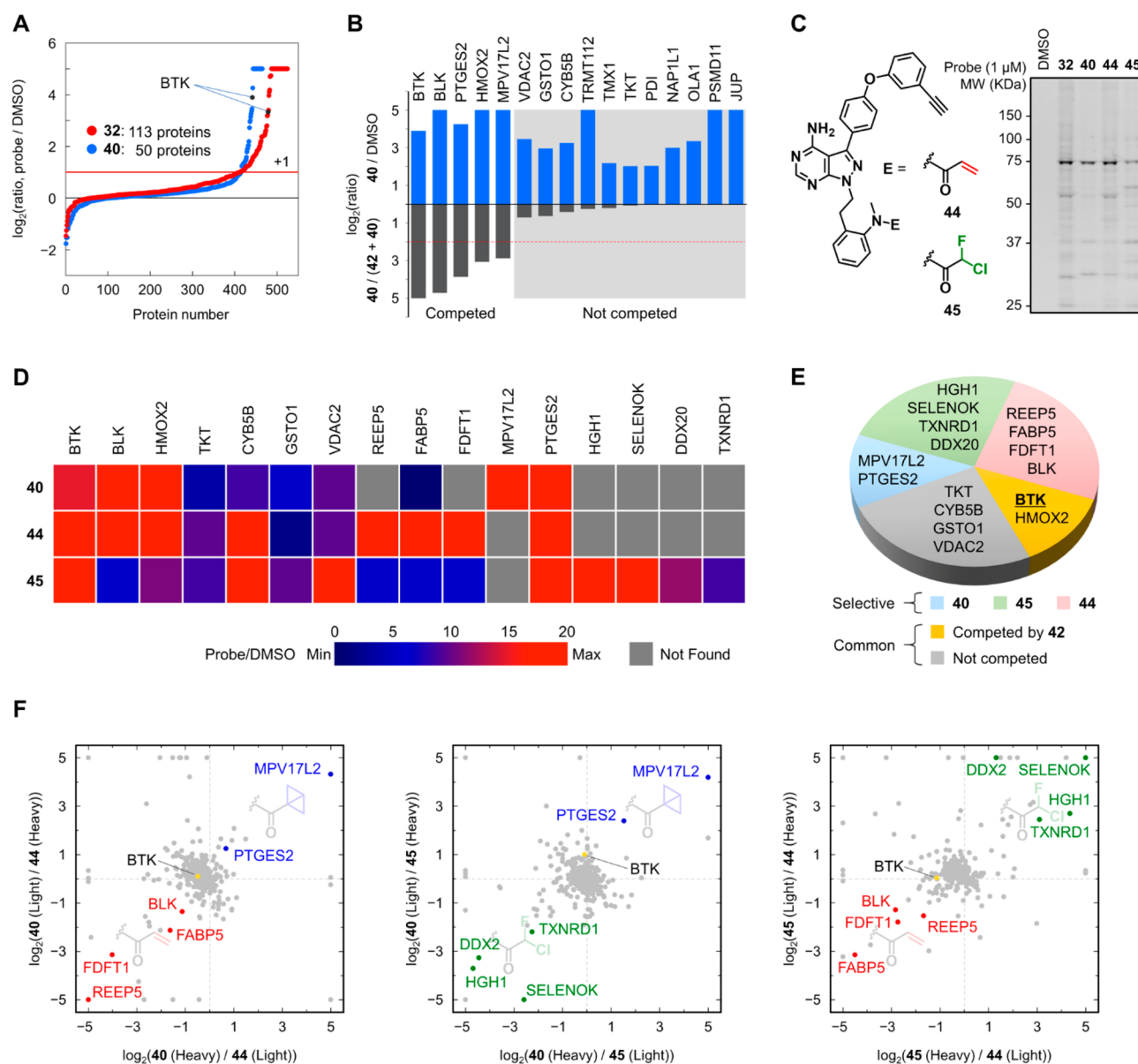


Figure 5. Proteome reactivity profiles of the covalent BTK probes. (A) SILAC ratio plots for proteins detected in probe-versus-DMSO (probe/DMSO) experiments. Ramos cells were treated with **32** or **40** ($1 \mu\text{M}$, 4 h). Results are plotted as \log_2 values of the median SILAC ratios obtained from triplicate mass spectrometry (MS) analyses of a single streptavidin-enriched sample. BTK is highlighted in black. (B) SILAC ratios of highly enriched proteins by probe **40** identified in the **40**/DMSO experiment and competition (DMSO + **40**)/(**42** + **40**) experiment. In the competition experiment, Ramos cells were pretreated with inhibitor **42** ($10 \mu\text{M}$, 1 h) or DMSO, followed by treatment with **40** ($1 \mu\text{M}$, 4 h). Results are plotted as \log_2 values of the median SILAC ratios obtained from triplicate MS analyses of a single streptavidin-enriched sample. Proteins with the **40**/DMSO ratio > 4 were displayed. (C) Reactivity profiles of the covalent BTK probes in Ramos cells ($1 \mu\text{M}$, 4 h) analyzed by in-gel ABPP. (D) Heatmap illustrating SILAC ratios of protein targets of **40**, **44**, and **45** obtained from the probe/DMSO experiments. Red represents the maximal ratio (20), and dark blue represents the minimal ratio. Gray designates proteins that were not enriched by the corresponding probe. (E) Classification of protein targets of **40**, **44**, and **45**. Green, blue, and red represent probe-selective targets of **45**, **40**, and **44**, respectively. Orange represents the common targets of the probes displaying ligand-dependent engagement with **40** as shown in (B). Gray represents common targets that were not competed by **42** as shown in (B). (F) Plots of SILAC ratio values of proteins in probe/probe competition experiments in combinations of **40** versus **44** (left), **40** versus **45** (middle), and **45** versus **44** (right). Results are plotted as \log_2 values of the median SILAC ratios obtained from triplicate MS analyses of a single streptavidin-enriched sample. BTK is highlighted in yellow. Probe-selective off-targets of **40**, **44**, and **45** are highlighted in blue, red, and green, respectively.

The concentration-dependent labeling experiment revealed that **40** efficiently reacted with BTK at a concentration of as low as $\sim 0.1 \mu\text{M}$, whereas **41** was less effective at the low concentration range (Figure 4B, middle panel). The covalent engagement of **40** with BTK was confirmed by the competitive labeling experiment, in which the major fluorescence band at 77 kDa selectively disappeared by the pretreatment of Ramos cells with an excess of ibrutinib ($10 \mu\text{M}$, 1 h) (Figure 4B, right panel). The

competitive labeling experiment also showed that the off-targets of **40** were not completely blocked by ibrutinib, suggesting that **40** possesses a unique off-target profile distinct from that of ibrutinib. The in-cell reaction kinetics study revealed that the initial reaction rate of **32** ($V_0 = 15.6 \times 10^{-2} \text{ min}^{-1}$) was much faster than that of **33** ($V_0 = 0.58 \times 10^{-2} \text{ min}^{-1}$) (Figure S6). However, the reaction kinetics greatly improved in **40** ($V_0 = 5.07 \times 10^{-2} \text{ min}^{-1}$), consistent with the observed higher reactivity of

the aromatic BCB amides **10** and **12** toward GSH as compared to that of the aliphatic BCB amide **15** (Figure 2B). The gel image shown in Figure 4B also suggested that BCB amide **40** displayed a higher target selectivity for BTK than did acrylamide **32** when both probes were used at a concentration of 1 μM . This trend in the selectivity was more clearly demonstrated by the in-gel ABPP analyses with the probes at higher concentrations (1–10 μM , 4 h) and under prolonged labeling time conditions (1 μM , 0.5–8 h) (Figure S7). The reactivity of the probes toward EGFR, another kinase target of acrylamide **32**,²⁷ was also examined (Figure S8). The in-gel ABPP analysis revealed that BCB amides **33** and **39–41** (5 μM , 4 h) exhibited a structure-dependent reactivity toward EGFR in A431 cells. The conjugation with EGFR was also observed in the labeling experiment using the cell lysate (1 μM , 1 h). The lower labeling efficiency of **40** as compared to that of acrylamide **32** implies the high target selectivity of **40** toward BTK. Nevertheless, these data suggest the potential utility of BCB amide as a covalent warhead for other protein kinases. The serum and microsomal stability tests revealed that BCB amides **33** and **40** exhibited stability comparable to that of **32**, suggesting that the BCB amide is not a metabolically unstable warhead (Figure S9).

The biological activity of the developed BCB amide-appended pyrazolopyrimidines was next evaluated (Figure 4C). The in vitro kinase inhibition assay showed that BCB amide **42**, a nonalkyne analogue of **40**, strongly inhibited the kinase activity of BTK ($\text{IC}_{50} = 17 \text{ nM}$). This inhibitory potency was much stronger than that of the nonreactive *tert*-butyl analogue **43** ($\text{IC}_{50} = 130 \text{ nM}$). In the cell-based assay, **42** inhibited autophosphorylation of BTK in the submicromolar range ($\text{IC}_{50} = 180 \text{ nM}$), whereas the activity of **43** was negligible ($\text{IC}_{50} > 20 \mu\text{M}$). Furthermore, **42** showed a weak inhibitory activity against autophosphorylation of the C481S mutant of BTK ($\text{IC}_{50} = 4.32 \mu\text{M}$). Taken together, these results strongly suggest that BCB amide **42** inhibited the kinase activity of BTK through the covalent modification of Cys481 in the ATP binding pocket. Ibrutinib is known as a remarkably potent BTK inhibitor²⁹ and showed ~ 50 -fold stronger activity than that of **42** in the in vitro kinase inhibitory assay (Figures 4C and S10). However, this difference in potency decreased to ~ 8 -fold in the context of the in-cell kinase inhibitory assay.

Chemical Proteomics. To quantitatively evaluate the proteome-wide reactivity of the covalent BTK probes, we performed chemoproteomic experiments using stable isotope labeling by amino acids in cell culture (SILAC) mass spectrometry combined with ABPP (Table S2).^{27,30} The initial experiment compared the isotopically labeled Ramos cells treated with BCB amide **40** or Michael acceptor **32** (1 μM , 4 h) to those treated with dimethyl sulfoxide (DMSO) (Figure 5A). The probe-labeled proteins in the combined whole cell lysates were conjugated to biotin-azide by CuAAC, enriched by streptavidin affinity purification, and identified and quantified by LC–MS. Probe-enriched proteins were defined as those that were detected three times across the MS analysis performed in triplicate and displayed median $\log_2(\text{probe}/\text{DMSO})$ values > 1 . We found that both probes **32** and **40** enriched targeted BTK with high $\log_2(\text{probe}/\text{DMSO})$ values of 3.33 and 3.89, respectively (Figure 5A). Both probes also enriched BLK, a tyrosine kinase belonging to the same TEC kinase family as BTK. Probe **40** enriched only these two kinases, whereas acrylamide **32** additionally enriched other protein kinases, such as MAP2K1 and MAP2K7. The total numbers of proteins enriched (probe/DMSO ratio > 2) by **32** and **40** were 113 and

50, respectively, suggesting the lower off-target activity of BCB amide **40** as compared to that of acrylamide **32**. Among the five protein targets of **32** in Ramos cells (BTK, BLK, TEC, CYB5B, and MAP2K7) reported by Cravatt et al.,²⁷ all but TEC were efficiently enriched by **32**, indicating that our results are in general consistent with those previously reported.

To characterize the off-targets of BCB amide, we next performed competition SILAC experiments with alkynylated BCB amide probe **40** and nonalkyne BCB amide **42**. Isotopically “light” and “heavy” cells were pretreated with **42** (10 μM , 1 h) or DMSO, respectively, followed by treatment with alkynylated probe **40** (1 μM , 4 h) (Figure 5B). Among the 16 proteins highly enriched by probe **40** ($40/\text{DMSO}$ ratio > 4), two kinases (BTK and BLK) and three nonkinase proteins (PTGES2, HMOX2, and MPV17L2) were strongly competed by the pretreatment with **42** ($(\text{DMSO} + 40)/(\text{42} + 40)$ ratio > 4), implying that their engagements with BCB amide were effectively induced by the reversible protein–ligand interactions. Among the identified proteins that were not competed by **42**, GSTO1 and TKT were reported to possess a highly reactive cysteine residue.³¹ In addition, CYB5B was annotated as a nonspecific protein target of the kinase inhibitor-based probes.²⁷

To gain more insight into how electrophilic moieties affect the proteome selectivity of the covalent ligands, we investigated the in-cell reactivity profiles of a series of BTK probes, **40**, **44**, and **45**, each bearing a different cysteine-reactive electrophile (BCB amide, acrylamide, and CFA, respectively) on the same ligand unit. In-gel ABPP analysis revealed that all of the probes reacted with BTK as the major target but the patterns of off-target bands were different, suggesting that the probes had unique proteome selectivities (Figures 5C and S11). We next performed the competitive SILAC experiments using three combinations of probes (**40/44**, **40/45**, and **45/44**). Each probe set was tested in two individual experiments at different isotopic labeling conditions (for example, **40** in “light” cells/**44** in “heavy” cells and **40** in “heavy” cells/**44** in “light” cells). The proteome reactivity profile of each probe was also investigated in the probe/DMSO SILAC experiments (Figures 5A and S12), and the highly enriched proteins (probe/DMSO ratio > 2) were identified. The combined analysis of the probe/probe competition and probe/DMSO experiments identified 16 proteins as probe targets (Figure 5D,E and Table S1). Among them, we identified six proteins as common targets, which were defined as those proteins commonly enriched by the three probes in the probe/DMSO experiments (probe/DMSO ratio > 2) but did not show apparent probe selectivity in the competition experiments (probe/probe ratio < 2). Of these, BTK and HMOX2 were likely to be ligand-selective targets, as the reaction of these proteins with BCB probe **40** was strongly competed by **42** (Figure 5B). The other four common targets (TKT, CYB5B, GSTO1, and VDAC2) were not strongly competed by **42**. We identified several proteins as probe-selective off-targets, which were selectively enriched by a single probe with a probe/probe ratio > 2 in the competition experiments (Figure 5E and F). By using this definition, we identified MPV17 mitochondrial inner membrane protein like 2 (MPV17L2) and prostaglandin E synthase 2 (PTGES2) as the selective off-targets of BCB amide **40**. Of note, MPV17L2 was exclusively enriched by **40** among the three probes. MPV17L2 is a mitochondrial inner membrane protein required for the assembly and stability of the mitochondrial ribosome.³² Although MPV17L2 has not been reported as a ligandable protein,^{8a,31} it contains several functionally uncharacterized

cysteines. PTGES2 was identified as another selective off-target of **42** by the competition experiments, although it was also enriched by two other probes in the probe/DMSO experiments (Figure 5D). We found four selective off-targets of acrylamide **44** (REEP1, FABP5, FDFT1, and BLK) and four selective off-targets of CFA **45** (HGH1, SELENOK, TXNRD1, and DDX20). These eight proteins displayed limited cross-reactivity across the three probes used (Figure 5D). Overall, our study clearly demonstrates that the proteome reactivity of the covalent ligands can be altered depending on the adopted electrophile.

CONCLUSION

Strain-enabled reactions have attracted much attention in recent years due to their versatility for constructing functional molecules with unique structural features, including drug candidates.^{18–22,33} In this Article, we have introduced BCB carboxylic amide as a new class of strained electrophiles that undergoes chemoselective reaction with cysteine thiol. We have shown that the thiol reactivity of BCB derivatives is highly tunable depending on the attached EWG. Among them, the aromatic BCB amides showed the moderate thiol reactivity that renders them suitable for use as TCI warheads. This reactivity profile of the BCB amide was successfully exploited for the development of a covalent inhibitor, with higher target selectivity toward BTK in human cells as compared to that of the acrylamide-based probe. We further revealed that the weakly reactive aliphatic BCB amides also could serve as covalent binders targeting BTK. Although their labeling efficiency was relatively low, we envision that the aliphatic BCB amide could be nonetheless useful in covalent drug design as a “latent” electrophile, which is inert in bulk water but activated in the binding pocket of the targeted protein.³⁴

Our chemical proteomic study using a series of BTK probes (**40**, **44**, and **45**) provided us with a new insight into the effect of the electrophiles on the off-target profiles of covalent ligands. We demonstrated that the proteome reactivity of the BTK probes could be altered considerably, depending on the adopted electrophiles. Of note, we identified several off-target proteins that selectively reacted with the individual probes. This finding suggests that the increase of the repertoire of the cysteine-reactive electrophiles would expand the range of covalent inhibitors with desired proteome reactivity profiles. A wide selection of such covalent inhibitors would help in avoiding unwanted off-target labeling of specific proteins and decrease the total number of off-targets.

ASSOCIATED CONTENT

Supporting Information

The Supporting Information is available free of charge at <https://pubs.acs.org/doi/10.1021/jacs.0c07490>.

Additional tables and figures as described in the text, experimental procedures, synthetic procedures, and spectral data of the target compounds (PDF)

Table S2: Full proteomic data set for ABPP-SILAC experiments (XLSX)

AUTHOR INFORMATION

Corresponding Authors

Naoya Shindo – Graduate School of Pharmaceutical Sciences, Kyushu University, Higashi-ku, Fukuoka 812-8582, Japan; orcid.org/0000-0002-2374-9896; Email: shindo708@phar.kyushu-u.ac.jp

Akio Ojida – Graduate School of Pharmaceutical Sciences, Kyushu University, Higashi-ku, Fukuoka 812-8582, Japan; orcid.org/0000-0002-9440-8167; Email: ojida@phar.kyushu-u.ac.jp

Authors

Keisuke Tokunaga – Graduate School of Pharmaceutical Sciences, Kyushu University, Higashi-ku, Fukuoka 812-8582, Japan

Mami Sato – Graduate School of Pharmaceutical Sciences, Kyushu University, Higashi-ku, Fukuoka 812-8582, Japan

Keiko Kuwata – Institute of Transformative Bio-Molecules (ITbM), Nagoya University, Nagoya, Aichi 464-8601, Japan

Chizuru Miura – Graduate School of Pharmaceutical Sciences, Kyushu University, Higashi-ku, Fukuoka 812-8582, Japan

Hirokazu Fuchida – Graduate School of Pharmaceutical Sciences, Kyushu University, Higashi-ku, Fukuoka 812-8582, Japan

Naoya Matsunaga – Graduate School of Pharmaceutical Sciences, Kyushu University, Higashi-ku, Fukuoka 812-8582, Japan

Satoru Koyanagi – Graduate School of Pharmaceutical Sciences, Kyushu University, Higashi-ku, Fukuoka 812-8582, Japan

Shigehiro Ohdo – Graduate School of Pharmaceutical Sciences, Kyushu University, Higashi-ku, Fukuoka 812-8582, Japan

Complete contact information is available at: <https://pubs.acs.org/10.1021/jacs.0c07490>

Notes

The authors declare no competing financial interest.

ACKNOWLEDGMENTS

This work was supported by a Grant-in-Aid for Scientific Research on Innovative Areas “Chemistry for Multimolecular Crowding Biosystems” (JSPS KAKENHI grant no. JP17H06349) and Platform Project for Supporting Drug Discovery and Life Science Research (Basis for Supporting Innovative Drug Discovery and Life Science Research (BINDS)) from AMED under grant number JP18am0101091. N.S. acknowledges Grant-in-Aid for Young Scientists B (JSPS KAKENHI grant no. JP17K15483), Grant-in-Aid for Scientific Research B (JSPS KAKENHI grant no. 19H02854), and AMED under grant no. JP20ak0101121 for their financial support. H.F. acknowledges JSPS Research Fellowships for Young Scientists. ITbM is supported by the World Premier International Research Center Initiative, Japan. K.K. acknowledges a Grant-in-Aid for Scientific Research on Innovative Areas (JSPS KAKENHI grant no. JP15H05955).

REFERENCES

- (1) (a) Potashman, M. H.; Duggan, M. E. Covalent Modifiers: An Orthogonal Approach to Drug Design. *J. Med. Chem.* **2009**, *52* (5), 1231–1246. (b) Singh, J.; Petter, R. C.; Baillie, T. A.; Whitty, A. The Resurgence of Covalent Drugs. *Nat. Rev. Drug Discovery* **2011**, *10* (4), 307–317. (c) Tamura, T.; Ueda, T.; Goto, T.; Tsukidate, T.; Shapira, Y.; Nishikawa, Y.; Fujisawa, A.; Hamachi, I. Rapid Labelling and Covalent Inhibition of Intracellular Native Proteins using Ligand-Directed N-Acyl-N-alkyl Sulfonamide. *Nat. Commun.* **2018**, *9*, 1870 DOI: [10.1038/s41467-018-04343-0](https://doi.org/10.1038/s41467-018-04343-0). (d) Chung, C. Y.-S.; Shin, H. R.; Berdan, C. A.; Ford, B.; Ward, C. C.; Olzmann, J. A.; Zoncu, R.; Nomura, D. K. Covalent targeting of the vacuolar H⁺-ATPase activates autophagy via mTORC1 inhibition. *Nat. Chem. Biol.* **2019**, *15* (8), 776–785.
- (2) (a) Thorarensen, A.; Martin, E.; Dowty, M.; Banker, M. E.; Juba, B.; Jason, J.; Lin, T.; Vincent, F.; Czerwinski, R. M.; Casimiro-Garcia, A.; Unwalla, R.; Trujillo, J. I.; Liang, S.; Balbo, P.; Che, Y.; Gilbert, A.

- M.; Matthew, F.; Brown, M. F.; Hayward, M.; Montgomery, J.; Leung, L.; Yang, X.; Soucy, S.; Hege, M.; Coe, J.; Langille, J.; Vajdos, F.; Chrencik, J.; Telliez, J.-B. Design of a Janus Kinase 3 (JAK3) Specific Inhibitor 1-((2S,5R)-5-((7H-Pyrrolo[2,3-d]pyrimidin-4-yl)amino)-2-methylpiperidin-1-yl)prop-2-en-1-one (PF-06651600) Allowing for the Interrogation of JAK3 Signaling in Humans. *J. Med. Chem.* **2019**, *60* (5), 1971–1993. (b) Quambusch, L.; Landel, I.; Depta, L.; Weisner, J.; Uhlenbrock, N.; Mglter, M. P.; Glanemann, F.; Althoff, K.; Siveke, J. T.; Rauh, D. Covalent-Allosteric Inhibitors to Achieve Akt Isoform-Selectivity. *Angew. Chem., Int. Ed.* **2019**, *58* (52), 18823–18829.
- (3) (a) Li, D.; Ambrogio, L.; Shimamura, T.; Kubo, S.; Takahashi, M.; Chiriac, L. R.; Padera, R. F.; Shapiro, G. I.; Baum, A.; Himmelsbach, F.; Rettig, W. J.; Meyerson, M.; Solca, F.; Greulich, H.; Wong, K.-K. BIBW2992, an Irreversible EGFR/HER2 Inhibitor Highly Effective in Preclinical Lung Cancer Models. *Oncogene* **2008**, *27* (34), 4702–4711. (b) Cross, D. A. E.; Ashton, S. E.; Ghiorghiu, S.; Eberlein, C.; Nebhan, C. A.; Spitzler, P. J.; Orme, J. P.; Finlay, M. R. V.; Ward, R. A.; Mellor, M. J.; Hughes, G.; Rahi, A.; Jacobs, V. N.; Brewer, M. R.; Ichihara, E.; Sun, J.; Jin, H.; Ballard, P.; Al-Kadhimi, K.; Rowlinson, R.; Klinowska, T.; Richmond, G. H. P.; Cantarini, M.; Kim, D.-W.; Ranson, M. R.; Pao, W. AZD9291, an Irreversible EGFR TKI, Overcomes T790M-Mediated Resistance to EGFR Inhibitors in Lung Cancer. *Cancer Discovery* **2014**, *4* (9), 1046–1061. (c) Finlay, M. R. V.; Anderton, M.; Ashton, S.; Ballard, P.; Bethel, P. A.; Box, M. R.; Bradbury, R. H.; Brown, S. J.; Butterworth, S.; Campbell, A.; Chorley, C.; Colclough, N.; Cross, D. A. E.; Currie, G. S.; Grist, M.; Hassall, L.; Hill, G. B.; James, D.; James, M.; Kemmitt, P.; Klinowska, T.; Lamont, G.; Lamont, S. G.; Martin, N.; McFarland, H. L.; Mellor, M. J.; Orme, J. P.; Perkins, D.; Perkins, P.; Richmond, G.; Smith, P.; Ward, R. A.; Waring, M. J.; Whittaker, D.; Wells, S.; Wrigley, G. L. Discovery of a Potent and Selective EGFR Inhibitor (AZD9291) of Both Sensitizing and T790M Resistance Mutations That Spares the Wild Type Form of the Receptor. *J. Med. Chem.* **2014**, *57* (20), 8249–8267.
- (4) Dahal, U. P.; Obach, R. S.; Gilbert, A. M. Benchmarking *In Vitro* Covalent Binding Burden As a Tool To Assess Potential Toxicity Caused by Nonspecific Covalent Binding of Covalent Drugs. *Chem. Res. Toxicol.* **2013**, *26* (11), 1739–1745.
- (5) (a) Baillie, T. A. Targeted Covalent Inhibitors for Drug Design. *Angew. Chem., Int. Ed.* **2016**, *55* (43), 13408–13421. (b) Liu, Q.; Sabnis, Y.; Zhao, Z.; Zhang, T.; Buhlage, S. J.; Jones, L. H.; Gray, N. S. Developing Irreversible Inhibitors of the Protein Kinase Cysteine. *Chem. Biol.* **2013**, *20* (2), 146–159.
- (6) (a) Honigberg, L. A.; Smith, A. M.; Sirisawad, M.; Verner, E.; Louny, D.; Chang, B.; Li, S.; Pan, Z.; Thamm, D. H.; Miller, R. A.; Buggy, J. J. The Bruton tyrosine kinase inhibitor PCI-32765 blocks B-cell activation and is efficacious in models of autoimmune disease and B-cell malignancy. *Proc. Natl. Acad. Sci. U. S. A.* **2010**, *107* (29), 13075–13080. (b) Byrd, J. C.; Harrington, B.; O'Brien, S.; Jones, J. A.; Schuh, A.; Devereux, S.; Chaves, J.; Wierda, W. G.; Awan, F. T.; Brown, J. R.; Hillmen, P.; Stephens, D. M.; Ghia, P.; Barrientos, J. C.; Pagel, J. M.; Woyach, J.; Johnson, D.; Huang, J.; Wang, X.; Kaptein, A.; Lannutti, B. J.; Covey, T.; Fardis, M.; McGreivy, J.; Hamdy, A.; Rothbaum, W.; Izumi, R.; Diacovo, T. G.; Johnson, A. J.; Furman, R. R. Acalabrutinib (ACP-196) in Relapsed Chronic Lymphocytic Leukemia. *N. Engl. J. Med.* **2016**, *374* (4), 323–332.
- (7) (a) Ostrem, J. M.; Peters, U.; Sos, M. L.; Wells, J. A.; Shokat, K. M. K-Ras(G12C) Inhibitors Allosterically Control GTP Affinity and Effector Interactions. *Nature* **2013**, *503* (7477), 548–551. (b) Zeng, M.; Lu, J.; Li, L.; Feru, F.; Quan, C.; Gero, T. W.; Ficarro, S. B.; Xiong, Y.; Ambrogio, C.; Paranal, R. M.; Catalano, M.; Shao, J.; Wong, K.-K.; Marto, J. A.; Fischer, E. S.; Jänne, P. A.; Scott, D. A.; Westover, K. D.; Gray, N. S. Potent and Selective Covalent Quinazoline Inhibitors of KRAS G12C. *Cell Chem. Biol.* **2017**, *24* (8), 1005–1016. (c) Janes, M. R.; Zhang, J.; Li, L.-S.; Hansen, R.; Peters, U.; Guo, X.; Chen, Y.; Babbar, A.; Firdaus, S. J.; Darjania, L.; Feng, J.; Chen, J. H.; Li, S.; Li, S.; Long, Y. O.; Thach, C.; Liu, Y.; Zariwala, A.; Ely, T.; Kucharski, J. M.; Kessler, L. V.; Wu, T.; Yu, K.; Wang, Y.; Yao, Y.; Deng, X.; Zarrinkar, P. P.; Brehmer, D.; Dhanak, D.; Lorenzi, M. V.; Hu-Lowe, D.; Patricelli, M. P.; Ren, P.; Liu, Y. Targeting KRAS Mutant Cancers with a Covalent G12C-Specific Inhibitor. *Cell* **2018**, *172* (3), 578–589. (d) Canon, J.; Rex, K.; Saiki, A. Y.; Mohr, C.; Cooke, K.; Bagal, D.; Gaida, K.; Holt, T.; Knutson, C. G.; Koppada, N.; Lanman, B. A.; Werner, J.; Rapaport, A. S.; San Miguel, T.; Ortiz, R.; Osgood, T.; Sun, J.-R.; Zhu, X.; McCarter, J. D.; Volak, L. P.; Houk, B. E.; Fakih, M. G.; O'Neil, B. H.; Price, T. J.; Falchook, G. S.; Desai, J.; Kuo, J.; Govindan, R.; Hong, D. S.; Ouyang, W.; Henary, H.; Arvedson, T.; Cee, V. J.; Lipford, J. R. The clinical KRAS^{G12C} inhibitor AMG 510 drives anti-tumor immunity. *Nature* **2019**, *575* (7781), 217–223. (e) Lanman, B. A.; Allen, J. R.; Allen, J. G.; Amegadzie, A. K.; Ashton, K. S.; Booker, S. K.; Chen, J. J.; Chen, N.; Frohn, M. J.; Goodman, G.; Kopecky, D. J.; Liu, L.; Lopez, P.; Low, J. D.; Ma, V.; Minatti, A. E.; Nguyen, T. T.; Nishimura, N.; Pickrell, A. J.; Reed, A. B.; Shin, Y.; Siegmund, A. C.; Tamayo, N. A.; Tegley, C. M.; Walton, M. C.; Wang, H.-L.; Wurz, R. P.; Xue, M.; Yang, K. C.; Achanta, P.; Bartberger, M. D.; Canon, J.; Hollis, L. S.; McCarter, J. D.; Mohr, C.; Rex, K.; Saiki, A. Y.; San Miguel, T.; Volak, L. P.; Wang, K. H.; Whittington, D. A.; Zech, S. G.; Lipford, J. R.; Cee, V. J. Discovery of a Covalent Inhibitor of KRAS^{G12C} (AMG 510) for the Treatment of Solid Tumors. *J. Med. Chem.* **2020**, *63* (1), 52–65. (f) Kettle, G. J.; Bagal, S. K.; Bickerton, S.; Bodnarchuk, M. S.; Breed, J.; Carbajo, R. J.; Cassar, D. J.; Chakraborty, A.; Cosulich, S.; Cumming, I.; Davies, M.; Eatherton, A.; Evans, L.; Feron, L.; Fillery, S.; Gleave, E. S.; Goldberg, F. W.; Harlfinger, S.; Hanson, L.; Howard, M.; Howells, R.; Jackson, A.; Kemmitt, P.; Kingston, J. K.; Lamont, S.; Lewis, H. J.; Li, S.; Liu, L.; Ogg, D.; Phillips, C.; Polanski, R.; Robb, G.; Robinson, D.; Ross, S.; Smith, J. M.; Tonge, M.; Whiteley, R.; Yang, J.; Zhang, L.; Zhao, X. Structure-Based Design and Pharmacokinetic Optimization of Covalent Allosteric Inhibitors of the Mutant GTPase KRAS^{G12C}. *J. Med. Chem.* **2020**, *63* (9), 4468–4483. (g) Fell, J. B.; Fischer, J. P.; Baer, B. R.; Blake, J. F.; Bouhana, K.; Briere, D. M.; Brown, K. D.; Burgess, L. E.; Burns, A. C.; Burkard, M. R.; Chiang, H.; Chicarelli, M. J.; Cook, A. W.; Gaudino, J. J.; Hallin, J.; Hanson, L.; Hartley, D. P.; Hicken, E. J.; Hingorani, G. P.; Hinklin, R. J.; Mejia, M. J.; Olson, P.; Otten, J. N.; Rhodes, S. P.; Rodriguez, M. E.; Savechenkov, P.; Smith, D. J.; Sudhakar, N.; Sullivan, F. X.; Tang, T. P.; Vigers, G. P.; Wollenberg, L.; Christensen, J. G.; Marx, M. A. Identification of the Clinical Development Candidate MRTX849, a Covalent KRAS^{G12C} Inhibitor for the Treatment of Cancer. *J. Med. Chem.* **2020**, *63* (13), 6679–6693.
- (8) (a) Backus, K. M.; Correia, B. E.; Lum, K. M.; Forli, S.; Horning, B. D.; Gonzalez-Paez, G. E.; Chatterjee, S.; Lanning, B. R.; Teijaro, J. R.; Olson, A. J.; Wolan, D. W.; Cravatt, B. F. Proteome-wide covalent ligand discovery in native biological systems. *Nature* **2016**, *534* (7608), 570–574. (b) Counihan, J. L.; Wiggenshorn, A. L.; Anderson, K. E.; Nomura, D. K. Chemoproteomics-Enabled Covalent Ligand Screening Reveals ALDH3A1 as a Lung Cancer Therapy Target. *ACS Chem. Biol.* **2018**, *13* (8), 1970–1977. (c) Resnick, E.; Bradley, A.; Gan, J.; Douangamath, A.; Krojer, T.; Sethi, R.; Geurink, P. P.; Aimon, A.; Amitai, G.; Bellini, D.; Bennett, J.; Fairhead, M.; Fedorov, O.; Gabizon, R.; Gan, J.; Guo, J.; Plotnikov, A.; Reznik, N.; Ruda, G. F.; Diaz-Saez, L.; Straub, V. M.; Sommer, T.; Velupillai, S.; Zaidman, D.; Zhang, Y.; Coker, A. R.; Dowson, C. G.; Barr, H. M.; Wang, C.; Huber, K. V. M.; Brennan, P. E.; Ova, H.; von Delft, F.; London, N. Rapid Covalent-Probe Discovery by Electrophile-Fragment Screening. *J. Am. Chem. Soc.* **2019**, *141* (22), 8951–8968.
- (9) (a) Shindo, N.; Fuchida, H.; Sato, M.; Watari, K.; Shibata, T.; Kuwata, K.; Miura, C.; Okamoto, K.; Hatsuyama, Y.; Tokunaga, K.; Sakamoto, S.; Morimoto, S.; Abe, Y.; Shiroishi, M.; Caaveiro, J. M. M.; Ueda, T.; Tamura, T.; Matsunaga, N.; Nakao, T.; Koyanagi, S.; Ohdo, S.; Yamaguchi, Y.; Hamachi, I.; Ono, M.; Ojida, A. Selective and Reversible Modification of Kinase Cysteines with Chlorofluoroacetamides. *Nat. Chem. Biol.* **2019**, *15* (3), 250–258. (b) Sato, M.; Fuchida, H.; Shindo, N.; Kuwata, K.; Tokunaga, K.; Guo, X.-L.; Inamori, R.; Hosokawa, K.; Watari, K.; Shibata, T.; Matsunaga, N.; Koyanagi, S.; Ohdo, S.; Ono, M.; Ojida, A. Selective Covalent Targeting of Mutated EGFR(T790M) with Chlorofluoroacetamide-Pyrimidines. *ACS Med. Chem. Lett.* **2020**, *11* (6), 1137–1144.
- (10) (a) Motiwala, H. F.; Kuo, Y.-H.; Stinger, B. L.; Palfey, B. A.; Martin, B. R. Tunable Heteroaromatic Sulfones Enhance in-Cell Cysteine Profiling. *J. Am. Chem. Soc.* **2020**, *142* (4), 1801–1810.

- (b) Zambaldo, C.; Vinogradova, E. V.; Qi, X.; Iaconelli, J.; Suci, R. M.; Koh, M.; Senkane, K.; Chadwick, S. R.; Sanchez, B. B.; Chen, J. S.; Chatterjee, A. K.; Liu, P.; Schultz, P. G.; Cravatt, B. F.; Bollong, M. J. 2-Sulfonylpyridines as Tunable, Cysteine-Reactive Electrophiles. *J. Am. Chem. Soc.* **2020**, *142* (19), 8972–8979.
- (11) Ma, N.; Hu, J.; Zhang, Z.-M.; Liu, W.; Huang, M.; Fan, Y.; Yin, X.; Wang, J.; Ding, K.; Ye, W.; Li, Z. 2*H*-Azirine-Based Reagents for Chemoselective Bioconjugation at Carboxyl Residues Inside Live Cells. *J. Am. Chem. Soc.* **2020**, *142* (13), 6051–6059.
- (12) Carvalho, L. A. R.; Almeida, V. T.; Brito, J. A.; Lum, K. M.; Oliveira, T. F.; Guedes, R. C.; Gonçalves, L. M.; Lucas, S. D.; Cravatt, B. F.; Archer, M.; Moreira, R. 3-Oxo- β -sultam as a Sulfonylating Chemotype for Inhibition of Serine Hydrolases and Activity-Based Protein Profiling. *ACS Chem. Biol.* **2020**, *15* (4), 878–883.
- (13) Lin, S.; Yang, X.; Jia, S.; Weeks, A. M.; Hornsby, M.; Lee, P. S.; Nichiporuk, R. V.; Iavarone, A. T.; Wells, J. A.; Toste, F. D.; Chang, C. J. Redox-based reagents for chemoselective methionine bioconjugation. *Science* **2017**, *355* (6325), 597–602.
- (14) Wiberg, K. B. The Concept of Strain in Organic Chemistry. *Angew. Chem., Int. Ed. Engl.* **1986**, *25* (4), 312–322.
- (15) Wiberg, K. B.; Lampman, G. M.; Ciula, R. P.; Connor, D. S.; Schertler, P.; Lavanish, J. Bicyclo[1.1.0]butane. *Tetrahedron* **1965**, *21* (10), 2749–2769.
- (16) Khoury, P. R.; Goddard, J. D.; Tam, W. Ring strain energies: substituted rings, norbornanes, norbornenes and norbornadienes. *Tetrahedron* **2004**, *60* (37), 8103–8112.
- (17) (a) Schneider, C.; Niisuke, K.; Boeglin, W. E.; Voehler, M.; Stec, D. F.; Porter, N. A.; Brash, A. R. Enzymatic synthesis of a bicyclobutane fatty acid by a hemoprotein-lipoxygenase fusion protein from the cyanobacterium *Anabaena* PCC 7120. *Proc. Natl. Acad. Sci. U. S. A.* **2007**, *104* (48), 18941–18945. (b) Chen, K.; Huang, X.; Kan, S. B. J.; Zhang, R. K.; Arnold, F. H. Enzymatic construction of highly strained carbocycles. *Science* **2018**, *360* (6384), 71–75.
- (18) Walczak, M. A. A.; Krainz, T.; Wipf, P. Ring-Strain-Enabled Reaction Discovery: New Heterocycles from Bicyclo[1.1.0]butanes. *Acc. Chem. Res.* **2015**, *48* (4), 1149–1158.
- (19) Fawcett, A.; Biberger, T.; Aggarwal, V. K. Carbopalladation of C-C σ -Bonds Enabled by Strained Boronate Complexes. *Nat. Chem.* **2019**, *11* (2), 117–122.
- (20) (a) Silvi, M.; Aggarwal, V. K. Radical Addition to Strained σ -Bonds Enables the Stereocontrolled Synthesis of Cyclobutyl Boronic Esters. *J. Am. Chem. Soc.* **2019**, *141* (24), 9511–9515. (b) Ociepa, M.; Wierzba, A. J.; Turkowska, J.; Gryko, D. Polarity-Reversal Strategy for the Functionalization of Electrophilic Strained Molecules via Light-Driven Cobalt Catalysis. *J. Am. Chem. Soc.* **2020**, *142* (11), 5355–5361.
- (21) (a) Blanchard, E. P., Jr.; Cairncross, A. Bicyclo[1.1.0]butane Chemistry. I. The Synthesis and Reactions of 3-Methylbicyclo[1.1.0]butanecarbonitriles. *J. Am. Chem. Soc.* **1966**, *88* (3), 487–495. (b) Gaoni, Y.; Tomažič, A. Bridgehead reactivity, nucleophilic and radical additions, and lithium aluminum hydride reduction of 1-(arylsulfonyl)bicyclobutanes: general access to substituted, functionalized cyclobutanes. Syntheses of (\pm)-citriol acetate, (\pm)-junione, and the tricyclo[3.3.0.0^{1,4}]octane and tricyclo[4.3.0.0^{1,7}]nonane ring systems. *J. Org. Chem.* **1985**, *50* (16), 2948–2957. (c) Gaoni, Y. Regiospecific additions of hydrazoic acid and benzylamine to 1-(arylsulfonyl)bicyclo[1.1.0]butanes. Application to the synthesis of *cis* and *trans* 2,7-methanoglutaric acids. *Tetrahedron Lett.* **1988**, *29* (13), 1591–1594. (d) Gaoni, Y. New bridgehead-substituted 1-(arylsulfonyl)bicyclo[1.1.0]butanes and some novel addition reactions of the bicyclic system. *Tetrahedron* **1989**, *45* (9), 2819–2840.
- (22) (a) Gianatassio, R.; Lopchuk, J. M.; Wang, J.; Pan, C.-M.; Malins, L. R.; Prieto, L.; Brandt, T. A.; Collins, M. R.; Gallego, G. M.; Sach, N. W.; Spangler, J. E.; Zhu, H.; Zhu, J.; Baran, P. S. Strain-release amination. *Science* **2016**, *351* (6270), 241–246. (b) Lopchuk, J. M.; Fjelbye, K.; Kawamata, Y.; Malins, L. R.; Pan, C.-M.; Gianatassio, R.; Wang, J.; Prieto, L.; Bradow, J.; Brandt, T. A.; Collins, M. R.; Elleraas, J.; Ewanicki, J.; Farrell, W.; Fadeyi, O. O.; Gallego, G. M.; Mousseau, J. J.; Oliver, R.; Sach, N. W.; Smith, J. K.; Spangler, J. E.; Zhu, H.; Zhu, J.; Baran, P. S. Strain-Release Heteroatom Functionalization: Development, Scope, and Stereospecificity. *J. Am. Chem. Soc.* **2017**, *139* (8), 3209–3226.
- (23) (a) McDonald, R. N.; Reitz, R. R. Strained Ring Systems. 16. Substituent Effects on the pKa Values of *cis*- and *trans*-1,2-Dimethyl-2-X-Cyclopropane-1-Carboxylic Acids and Related Bicyclo[n.1.0]-Alkane-1-Carboxylic Acids. *J. Am. Chem. Soc.* **1976**, *98* (25), 8144–8155. (b) Amey, R. L.; Smart, B. E. Bicyclo[1.1.0]butanes. Reactions with cyclic azo compounds. *J. Org. Chem.* **1981**, *46* (20), 4090–4092. (c) Schwartz, B. D.; Zhang, M. Y.; Attard, R. H.; Gardiner, M. G.; Malins, L. R. Structurally Diverse Acyl Bicyclobutanes: Valuable Strained Electrophiles. *Chem. - Eur. J.* **2020**, *26* (13), 2808–2812.
- (24) Wiberg, K. B.; Ciula, R. P. Ethyl Bicyclo[1.1.0]butane-1-carboxylate. *J. Am. Chem. Soc.* **1959**, *81* (19), 5261–5262.
- (25) Hoz, S.; Azran, C.; Sella, A. Atomic Motions and Protonation Stereochemistry in Nucleophilic Additions to Bicyclobutanes. *J. Am. Chem. Soc.* **1996**, *118* (23), 5456–5461.
- (26) Azran, C.; Hoz, S. Bridgehead Substituents Effect on the Reactivity of Bicyclobutane in its Reactions with Nucleophiles. A Comparison with Olefinic Systems. *Tetrahedron* **1995**, *51* (42), 11421–11430.
- (27) Lanning, B. R.; Whitby, L. R.; Dix, M. M.; Douhan, J.; Gilbert, A. M.; Hett, E. C.; Johnson, T. O.; Joslyn, C.; Kath, J. C.; Niessen, S.; Roberts, L. R.; Schnute, M. E.; Wang, C.; Hulce, J. J.; Wei, B.; Whiteley, L. O.; Hayward, M. M.; Cravatt, B. F. A road map to evaluate the proteome-wide selectivity of covalent kinase inhibitors. *Nat. Chem. Biol.* **2014**, *10* (9), 760–767.
- (28) An ab initio study has suggested that nucleophilic additions to BCB derivatives prefer an equatorial approach to the central bond: Hoz, S. Cyclobutane-Bicyclobutane System-6 An *Ab Initio* Calculation of the Preferred Pathway for Nucleophilic Attack on Bicyclobutane. *Tetrahedron* **1984**, *40* (24), 5213–5216.
- (29) Chen, J.; Kinoshita, T.; Gururaja, T.; Sukbuntherng, J.; James, D.; Lu, D.; Whang, J.; Versele, M.; Chang, B. Y. The effect of Bruton's tyrosine kinase (BTK) inhibitors on collagen-induced platelet aggregation, BTK, and tyrosine kinase expressed in hepatocellular carcinoma (TEC). *Eur. J. Haematol.* **2018**, *101* (5), 604–612.
- (30) Niessen, S.; Dix, M. M.; Barbas, S.; Potter, Z. E.; Lu, S.; Brodsky, O.; Planken, S.; Behenna, D.; Almaden, C.; Gajiwala, K. S.; Ryan, K.; Feree, R.; Lazear, M. R.; Hayward, M. M.; Kath, J. C.; Cravatt, B. F. Proteome-wide Map of Targets of T790M-EGFR-Directed Covalent Inhibitors. *Cell Chem. Biol.* **2017**, *24* (11), 1388–1400.
- (31) Weerapana, E.; Wang, C.; Simon, G. M.; Richter, F.; Khare, S.; Dillon, M. B.; Bachovchin, D. A.; Mowen, K.; Baker, D.; Cravatt, B. F. Quantitative reactivity profiling predicts functional cysteines in proteomes. *Nature* **2010**, *468* (7325), 790–795.
- (32) Dalla Rosa, I.; Durigon, R.; Pearce, S. F.; Rorbach, J.; Hirst, E. M.; Vidoni, S.; Reyes, A.; Brea-Calvo, G.; Minczuk, M.; Woellhaf, M. W.; Herrmann, J. M.; Huynen, M. A.; Holt, I. J.; Spinazzola, A. MPV17L2 is required for ribosome assembly in mitochondria. *Nucleic Acids Res.* **2014**, *42* (13), 8500–8515.
- (33) (a) Kanazawa, J.; Maeda, K.; Uchiyama, M. Radical Multi-component Carboamination of [1.1.1]Propellane. *J. Am. Chem. Soc.* **2017**, *139* (49), 17791–17794. (b) Fawcett, A.; Murtaza, A.; Gregson, C. H. U.; Aggarwal, V. K. Strain-Release-Driven Homologation of Boronic Esters: Application to the Modular Synthesis of Azetidines. *J. Am. Chem. Soc.* **2019**, *141* (11), 4573–4578. (c) Zhang, X.; Smith, R. T.; Le, C.; McCarver, S. J.; Shireman, B. T.; Carruthers, N. I.; MacMillan, D. W. C. Copper-mediated synthesis of drug-like bicyclopentanes. *Nature* **2020**, *580* (7802), 220–226.
- (34) (a) Mons, E.; Jansen, I. D. C.; Loboda, J.; van Doodewaerd, B. R.; Hermans, J.; Verdoes, M.; van Boeckel, C. A. A.; van Veelen, P. A.; Turk, B.; Turk, D.; Ovaa, H. The Alkyne Moiety as a Latent Electrophile in Irreversible Covalent Small Molecule Inhibitors of Cathepsin K. *J. Am. Chem. Soc.* **2019**, *141* (8), 3507–3514. (b) Mortenson, D. E.; Brighty, G. J.; Plate, L.; Bare, G.; Chen, W.; Li, S.; Wang, H.; Cravatt, B. F.; Forli, S.; Powers, E. T.; Sharpless, K. B.; Wilson, I. A.; Kelly, J. W. Inverse Drug Discovery” Strategy to Identify Proteins That Are Targeted by Latent Electrophiles as Exemplified by Aryl Fluorosulfates. *J. Am. Chem. Soc.* **2018**, *140* (1), 200–221.